Title

Dormancy dynamics and dispersal contribute to soil microbiome resilience

Authors

Jackson W Sorensen[a] and Ashley Shade[a,b,c]

[a]Department of Microbiology and Molecular Genetics, Michigan State University, East Lansing, MI 48824

[b] Department of Plant, Soil and Microbial Sciences, Michigan State University, East Lansing, MI 48824 USA

[c]Program in Ecology, Evolutionary Biology and Behavior, Michigan State University, East Lansing

Abstract

In disturbance ecology, stability is composed of resistance to change and resilience towards recovery after the disturbance subsides. Two key microbial mechanisms that can support microbiome stability include dormancy and dispersal. Specifically, microbial populations that are sensitive to disturbance can be re-seeded by local dormant pools of viable and reactivated cells, or by immigrants dispersed from regional metacommunities. However, it is difficult to quantify the contributions of these mechanisms to stability without, first, distinguishing the active from inactive membership, and, second, distinguishing the populations recovered by

local resuscitation from those recovered by dispersed immigrants. Here, we investigate the contributions of dormancy dynamics (activation and inactivation), and dispersal to soil microbial community resistance and resilience. We designed a replicated, 45-week time-series experiment to quantify the responses of the active soil microbial community to a thermal press disturbance, including unwarmed control mesocosms, disturbed mesocosms without dispersal, and disturbed mesocosms with dispersal after the release of the stressor. Communities changed in structure within one week of warming. Though the disturbed mesocosms did not fully recover within 29 weeks, resuscitation of thermotolerant taxa was key for community transition during the press, and both resuscitation of opportunistic taxa and immigration contributed to community resilience. Also, mesocosms with dispersal were more resilient than mesocosms without. This work advances the mechanistic understanding of how microbiomes respond to disturbances in their environment.

Keywords

Stability, disturbance ecology, recovery, resuscitation, 16S rRNA: rRNA gene, metagenomics, microbial ecology, community assembly, press disturbance, resistance, metacommunity, immigration

Introduction

Ongoing changes to Earth's climate are projected to alter disturbance regimes and to pervasively expose ecosystems to stressors like elevated atmospheric greenhouse gases and increased temperatures[1]. Microbial communities, or *microbiomes*, provide vital ecosystem functions and are key players in determining ecosystem responses to environmental changes[2,3]. Understanding the mechanisms that underpin microbiome responses to environmental disturbances will support efforts to predict, and, potentially, manage, microbiomes for stable functions within their ecosystems.

In disturbance ecology, stability refers to consistent properties in the face of a stressor [4]. Here, we apply terms from disturbance ecology as they have been adopted in microbial ecology[5–7]. Stability includes components of both resistance and resilience. Resistance is the capacity of a system to withstand change in the face of a stressor, and its inverse is sensitivity. Resilience is the extent to which a system recovers following a disturbance, and is often expressed as a rate of change over time. Secondary succession is the process of community reassembly after a disturbance, and it can lead to either a state of recovery or an alternative stable state. Recovery is when a system fully returns to either its pre-disturbance state or is indistinguishable from a comparative control, and this term can be applied both to the state of the stressor and to the responsive community. Similarly, an alternative stable state is when the system does not return but rather assumes a different state. Together, resistance and resilience are the major quantifiable components of stability, and they can be calculated from community measurements of alpha diversity, beta diversity, or function[6,8].

There are two related microbial mechanisms that support population persistence in the face of disturbance, and therefore contribute to community resistance, resilience, and recovery. One mechanism is microbial dispersal, as successful immigrants can support resilience and recovery of sensitive populations. Across an interconnected landscape, microbial metacommunities are linked via dispersal, and so immigrants originate from the regional species pool [9–12]. A second important but less-considered mechanism is microbial dormancy dynamics [13,14]. Dormancy dynamics include initiation and resuscitation. Initiation into dormancy can support local survival of populations sensitive to the disturbance, and therefore support community resistance by stabilizing community structure. Resuscitation from dormancy can support resilience and recovery by re-seeding sensitive populations from the local dormant pool. Thus, while both dispersal and resuscitation can support microbiome stability, dispersed immigrants originate regionally while resuscitated members originate locally. After a disturbance, if sensitive populations are not repopulated via immigration or resuscitation, they will become locally extinct and contribute to necromass (aka relic DNA, [15]).

We designed a replicated time-series experiment to quantify the contributions of dormancy dynamics and dispersal to the response of a soil microbiome to a thermal press disturbance. We targeted a soil microbiome because terrestrial microbiomes are front-line responders to climate change and sequesters of carbon [2,3], and therefore an important constituent to understand for predicting ecosystem outcomes to environmental change. Also, soils harbor the highest known microbial diversity [16–18] and present a maximum challenge in deciphering microbiome responses to disturbance. Furthermore, a majority of the microbial

cells or richness in soil is dormant [13,19], reportedly as high as 80%, representing a considerable pool of microbial functional potential. Finally, across heterogeneous soils, an average of 40% of the microbiome DNA was necromass that existed extracellularly[15]. This suggests that DNA-based methods of determining microbiome dynamics include both inactive and necromass reservoirs, and that there is need for increased precision to move forward to quantify mechanisms underpinning microbiome stability.

The mesocosm experiment reported here follows prior field work in Centralia, Pennsylvania [20–24]. Centralia is the site of an underground coal seam fire that ignited in 1962 and advances 5-7 my^{-1} along the coal seams[25,26]. The coal seams are highly variable in depth, but average 70 m below the surface[25], so as the fire advances underground it warms the overlying surface soils from ambient to mesothermal to thermal conditions . After the fire advances, previously warmed soils cool to ambient temperatures. In the field, we observed that previously warmed soils recovered towards reference soils in bacterial and archaeal community structure, with the exception of a slightly increased selection for Acidobacteria in the recovered soils (attributable to lower soil pH after coal combustion,[20]). However, during fire impact, there was high divergence among soil communities, and we hypothesized that differences in dormancy dynamics (e.g., different members resuscitating and initiating priority effects during the stress) may explain the divergences. We also hypothesized that resuscitation would shift community structure during the thermal disturbance, but that resuscitation and dispersal would together support resilience after the disturbance subsided. Therefore, in this experiment, we aimed to control dispersal, and also to quantify activity dynamics and determine their consistency and test our hypotheses.

Materials and Methods

Soil collection, mesocosm design, and soil sampling

Eight kg of soil was collected in Whirlpack bags from the top ten centimeters of a reference site in Centralia, PA (site C08, 40 48.084N 076 20.765W) on March 31st, 2018. The site is temperate with the following chemical-physical properties: Organic Matter 4.8%; Nitrate 7.9 ppm; Ammonium 20.5 ppm; pH 5; Sulfur 19 ppm; Potassium 69 ppm; Calcium 490 ppm, Magnesium 59 ppm; Iron 110 ppm, and Phosphorus 395 ppm. The ambient soil temperature when collected was 4°C. The sample was stored at 4°C until the experiment was initiated. Soil was sieved through a 4mm mesh, homogenized, and ~300 g were dispensed into 15 autoclaved quart-sized glass canning jars that were used as mesocosms (Ball). The homogenized soil sample intentionally was used in all 15 mesocosms to assess the reproducibility of community temporal dynamics starting from the same soil source. Percent soil moisture was determined using by massing and drying. Each mesocosm was massed weekly to assess evaporation and any loss of water mass was replaced with sterile water to maintain percent soil moisture throughout the experiment. Sterile metal canning lids were secured loosely to prevent anaerobiosis. All set-up and manipulation of the mesocosms was performed in a Biosafety Level 2 cabinet (ThermoScientific 1300 Series A2) and we used aseptic technique.

Mesocosms first were acclimated at 14°C to mimic the ambient soil temperature at the typical time of fall soil collection and to coordinate with our previous field study [20]. Acclimation proceeded for four weeks in a cooling incubator (Fischer Scientific Isotemp), and then soils were divided into three treatment groups (**Figure 1**). Six unwarmed control

mesocosms (“Control”) were maintained at 14°C for the duration of the experiment. Nine warmed mesocosms (“Disturbance”) were subjected to a 12-week disturbance regime to simulate a press thermal disturbance. First, the temperature was gradually increased to 60°C, by 3°C to 3.5°C daily increments over two weeks. Second, the temperature was maintained at 60°C for 8 weeks. Sixty degrees was chosen because it was close to the observed maximum thermal temperature that we have measured in surface soils impacted by the Centralia coal seam fire [20]. Next, the temperature was gradually decreased to 14°C, by 3°C to 3.5°C daily increments over two weeks. Finally, the mesocosms were maintained at 14°C for four weeks until the penultimate sampling. From the nine disturbed mesocosms, four were randomly selected for the dispersal treatment (“Disturbance + Immigration”). These four disturbed mesocosms received a dispersal event one week after the temperature was recovered to 14°C after the thermal disturbance. Each was inoculated with 0.5 mL of a 10% weight by volume soil slurry made from a composite soil sample from the six unwarmed control mesocosms, and then gently mixed with a sterile spatula. Using qPCR data from control mesocosms at week 16, we estimate that approximately 6.37×10^6 cells were dispersed into each Disturbance + Immigration mesocosm. We used soil from the control mesocosms to simulate dispersal from similar, adjacent soils to repopulate disturbed communities, as expected in the field. Finally, all mesocosms were left undisturbed at 14°C for another 25 weeks prior to the final 45-week sampling. During the final 25-week incubation, percent moisture was not monitored.

Mesocosms were non-destructively sampled after 4, 5, 6, 10, 14, 15, 16, 20, and 45 weeks of incubation. At each time point, approximately 15 g soil was removed from a

mesocosm, of which ~13 g was flash-frozen in liquid nitrogen for RNA preservation and stored at -80°C until RNA/DNA co-extraction.

RNA/DNA co-extraction

To obtain RNA and DNA from the same cell pool, we minimally modified a manual coextraction protocol originally published by [27]. For each sample, 0.5 g of flash-frozen soil was added to Qiagen PowerBead Tubes containing 0.70 mm garnet beads. Next, 500 uL of a 5% CTAB/Phosphate buffer and 500 uL of phenol:chloroform:isoamyl alcohol were added to each PowerBead tube. Cells were then lysed using a Model 607 MiniBeadBeater-16 (BioSpec Products Inc.) for 30 seconds, followed by a 10 min centrifugation at 10,000 x g and 4°C. The top aqueous layer was transferred to a fresh tube and 500 uL chloroform:isoamyl alcohol was added. The tubes were inverted several times to form an emulsion before a five minute centrifugation at 16,000 x g and 4°C. The top aqueous layer was transferred to a clean 1.5 mL centrifuge tube. Nucleic acids were precipitated by adding two volumes of a 30% PEG6000 1.6M NaCL solution, inverting several times to mix, and incubating on ice for two hours. After incubation, nucleic acids were pelleted by a 20 min centrifugation at 16,000 x g and 4°C. The supernatant was removed from each tube and one mL of ice-cold ethanol was added to the pelleted nucleic acids. Tubes were centrifuged for 15 min at 16,000 x g and 4°C, and the ethanol supernatant was removed. Pelleted nucleic acids were left to air dry before resuspending in 30 uL of sterile DEPC-treated water.

To purify the RNA, co-extracted nucleic acids were diluted 1:100 before treatment with Ambion Turbo DNA-free DNase kit, using the robust treatment option in the manufacturer's

instructions. Extracted nucleic acids were mixed with 0.1 volumes of the 10X Turbo DNase Buffer and three uL of TURBO Dnase enzyme (six units total) and incubated at 37°C for 30 min. After incubation, 0.2 volumes of DNase inactivation reagent was added and incubated for five minutes at room temperature before a five min centrifugation at 2,000 x g and room temperature. The treated supernatant was removed and used as the template for reverse transcription. RNA purity was assessed by PCR (see below for details) and showed no amplification. Reverse transcription was performed with random hexamers using the SuperScript III First-Strand Synthesis System for RT-PCR(Invitrogen) per manufacturer's instructions.

PCR of cDNA and no-RT controls was performed using the Earth Microbiome Project 16S rRNA gene V4 primers(515F 5'-GTGCCAGCMGCCGCGGTAA-3', 806R 5'-GGACTACHVGGGTWTCTAAT-3') [16,28]. Temperature cycling was as follows: 94°C for four minutes followed by 30 cycles of 94°C for 45 seconds, 50°C for 60 seconds and 72°C for 90 seconds followed by a final elongation step at 72°C for 10 minutes. Products were visualized using gel electrophoresis.

16S rRNA and 16S rRNA gene sequencing and processing

Here, for simplicity we use "microbiome" to refer to the bacterial and archaeal community members captured by amplifying and Illumina sequencing of the 16S ribosomal RNA and DNA (rRNA gene). Library preparation and sequencing was performed by the Michigan State University Genomics Core Research Facility. A single library was prepped using the method in Kozich et al (2013) [29]. PCR products were normalized using Invitrogen SequalPrep DNA

Normalization Plates. This library was loaded onto 4 separate Illumina MiSeq V2 Standard flow cells and sequenced using 250bp paired end format with a MiSeq V2 500 cycle reagent cartridge. Base calling was performed by the Illumina Real Time Analysis (RTA) V1.18.54.

All samples were first checked for any contaminating primer sequences using cutadapt[30], before being processed together using the USEARCH pipeline[31,32]. Briefly, paired end reads were merged using -fastq_mergepairs and then dereplicated using -fastx_uniques. Reads were clustered *de novo* at 97% identity and then the original merged reads were mapped to the representative sequences of each cluster. Each OTU was classified using SINTAX[33] and with the Silva database (version 123, [34]).

Designating Total and Active Communities

Each RNA and DNA sample was rarefied to 50,000 reads in R using the vegan package version 2.5-4 [35] discarding any samples which did not contain sufficient reads (**Figure S1**). Samples for which either the RNA or DNA did not have 50,000 reads were omitted from the analysis presented here (12 out of 135 in total). The Total community was defined as the community recovered in the DNA reads. The Active community was defined per sample, using the DNA read numbers of those taxa that had 16S rRNA:rRNA gene ratio was >1 in each sample[36]. Consequently, while every sample was initially rarefied to 50,000 reads, each sample's active community varied slightly in total reads. Finally, we did not include taxa that had undefined rRNA:rRNA gene ratios ("phantoms") in the analysis (**Figure S2**, see discussion in supplementary materials).

Quantitative PCR (qPCR)

qPCR was performed on the V4 region of the 16S rRNA gene and conducted in a BioRad CFX qPCR machine using the Absolute QPCR Mix, SYBR Green, no ROX (Thermo Scientific). Each reaction contained 12.5ul of the 2X Absolute QPCR Mix, 1.25 ul each of 10uM primers 515F and 806R, 3uL of template DNA and 2uL of PCR grade water. Temperature cycling conditions were as follows: 15 minutes at 95°C, followed by 39 cycles of 94°C for 45 seconds, 50°C for 60 seconds, and 72°C for 90 seconds, followed by a final elongation step at 72°C for 10 minutes. Fluorescence was measured in each well at the end of every cycle. Extracted gDNA from *E. coli* MG1655 was used for the standard curve, and was run in triplicate with every plate. Samples were run in duplicate across different plates and those that amplified after the lowest point of the standard curve (27 copies per reaction) were treated as zeroes. No template controls were included in every qPCR plate and they never amplified. Amplification specificity was assessed by melt curve (60°C to 95°C, 0.5°C increments).

Calculating resistance and resilience of community structure

We calculated resistance and resilience as described in Shade and Peter 2012[6] and Orwin and Wardle 2004 [8]. These are unitless metrics that have a theoretical range from -1 to 1. Resistance of the active community structure at week 10 was calculated for every disturbed mesocosm using Equation 1:

Eq. 1

$$\mathrm{RS} = 1 - \frac{2*|y_c - y_d|}{y_c + |y_c - y_d|}$$

238 , where y_c is the mean Bray Curtis similarity for Control mesocosms at week 10 compared to
239 week 4 (pre-disturbance), and y_d is the individually calculated Bray Curtis similarity of each
240 disturbed mesocosm at week 10 to week 4. Resilience of the active community in each
241 disturbed mesocosm was calculated for the observed secondary succession (week 16 to 45) as
242 well as the initial (week 16 to 20) and the long-term (week 20 to 45) secondary succession using
243 Equation 2.

244 Eq 2.

245 $$\mathrm{RL} = \frac{2 * |\mathrm{y_{c,s}} - \mathrm{y_{d,s}}|}{(|\mathrm{y_{c,s}} - \mathrm{y_{d,s}}| + |\mathrm{y_{c,e}} - \mathrm{y_{d,e}}|)} - 1$$

246

247 , where *s* is the start of the secondary succession and *e* is the end, $y_{c,s}$ is the mean Bray Curtis
248 similarity of Control mesocosms at week *S* to week 4 (pre-disturbance), $y_{d,s}$ is the Bray Curtis
249 similarity of each disturbed mesocosm at week S to week 4 (pre-disturbance), $y_{c,e}$ is the mean
250 Bray Curtis similarity of Control mesocosms at week *e* to week 4, and $y_{d,e}$ is the Bray Curtis
251 similarity of each disturbed mesocosms at week *e* to week 4.

252

253 *Ecological statistics*

254 Ecological analyses were performed in R[37]. The adonis and anosim function in the
255 vegan package was used to perform PERMANOVAs[38] and ANOSIM respectively, to assess
256 disturbance and immigration effects on community composition, and the betadisper function
257 was used to quantify beta dispersion[39] with Tukey's Honestly Significant Difference post-hoc
258 test across Control, Disturbance, and Disturbance + Immigration treatments. Pairwise tests for
259 alpha diversity (Richness and Pielou's Evenness), community size (i.e. 16S rRNA gene copies per

gram of soil), and resilience values were performed using the Kruskal-Wallis test, with Dunn's post-hoc correction for multiple comparisons when needed to assess differences between control, disturbance, and immigration treatments. Principal coordinates analysis was used for ordination of pairwise sample differences based on Bray-Curtis dissimilarity. Procrustes superimposition (PROTEST) was performed using the procrustes function in the vegan package to compare community structure trajectories in direction and extent of change and a false discovery rate adjustment was used for multiple tests. Data visualizations were performed using ggplot2[40]. Heatmaps were made using the heatmap.2 function in the gplots package[41].

To understand potential roles of dormancy initiation and resuscitation in driving community resistance and resilience, we distinguished between taxa that changed in their activity from taxa that changed in their detection over the course of the disturbance. Taxa that fell below detection (there was no rRNA gene detected in a particular sample) were coded differently for the heatmap than taxa that became inactive (rRNA:rRNA gene shifted from > 1 to < 1). For the heatmap, we used the Active community for the input data, but coded taxa that fell below detection in the Total community as NAs to distinguish them from inactive taxa, which were coded as 0. Notably, taxa that fell below detection in the Total community could have been either active, inactive, or locally extinct. To conservatively attribute activity dynamics, we restricted the heatmap visualization only to the taxa that were among the 50 most abundant in Active samples over the course of the experiment.

Responsive taxa were those that changed in activity over secondary succession (between weeks 16, 20, and 45) by their 16S rRNA:rRNA gene ratio, either from < 1 to > 1 or > 1

to < 1. Immigrant taxa were undetected in all disturbed mesocosms at week 16, but detected in Control mesocosms at Week 16 and Disturbance + Immigration mesocosms at either week 20 or week 45 while remaining undetected in the Disturbance mesocosms. Contributions of responsive and immigrant taxa to beta diversity were calculated as the Bray-Curtis dissimilarity attributed to the responsive taxa subset and divided by the total Bray-Curtis dissimilarity, both calculated from the Total (DNA) community, as done previously to assess the contributions of conditionally rare taxa [42] and the contributions of core taxa [43] to beta diversity. Briefly, to calculate the proportional contribution of any subset of taxa to observed Bray Curtis similarity, the Bray-Curtis dissimilarity attributable to the subset of taxa is divided by the total Bray-Curtis dissimilarity calculated from the entire community. Because Bray-Curtis dissimilarity is the sum of the difference in abundances of taxa in two communities divided by the total abundance of the taxa in those two communities, one can calculate the contribution of a subset of taxa to the Bray-Curtis dissimilarity by only including the subset in the numerator while including the total community in the denominator. This approach is transferable to other resemblance metrics and not restricted to use with Bray-Curtis. The detailed code for this calculation is available on GitHub.

Data availability and code

Sequence workflows, OTU tables, and statistical workflows to reproduce the analyses described here are available on GitHub (https://github.com/ShadeLab/PAPER_Sorensen_PhilTransB_2020). All raw sequence data are deposited in the NCBI Short Read Archive under BioProject PRJNA559185.

304

305 Results

306 *Sequencing summary*

307 In total, we sequenced 135 pairs of samples (cDNA and DNA) across nine timepoints and
308 15 mesocosms. We rarefied all samples to 50,000 reads, and removed those samples with
309 fewer than 50,000 reads. This resulted in the removal of 12 samples and left 53 unwarmed
310 Control, 36 Disturbance, and 34 Disturbance + Immigration pairs of samples. After rarefaction,
311 sample richness ranged from 84 to 4,108, with 16,854 total OTUs observed, inclusive of both
312 DNA and RNA datasets.

313

314 *Overarching responses to the thermal press disturbance*

315 Total community richness responded consistently and as expected to the thermal press
316 disturbance. There was a notable bottle effect of maintaining field soil in mesocosms, indicated
317 by the gradual decrease in richness over time in the unwarmed Control treatment (**Figure 2AB**).
318 In the Disturbance treatment, there was a modest but statistically supported decrease in
319 richness one week after warming from 14°C to 37 °C (week 5 all Disturbance v. Control
320 comparison, Kruskal-Wallis test, $p = 0.003$), and then a more substantial decrease after
321 warming to 60°C at week 6 (Kruskal-Wallis test, $p = 0.002$). Disturbance community size
322 decreased over weeks four to seven and then maintained at a median of 1.03×10^7 rRNA gene
323 copies per g soil (**Figure 3**). Control communities decreased until week seven (bottle effect) and
324 then increased rapidly by week ten and generally stabilized at median of 2.98×10^8 16S rRNA
325 gene copies/g soil (**Figure 3A**). Together, these results show that the warming treatment acted

as an environmental filter, resulting either in death or population decreases past the limits of detection for taxa that were otherwise fit in unwarmed conditions. Furthermore, there was a weak increase in richness after the dispersal event in the Disturbance + Immigration treatment, relative to the Disturbance treatment (Kruskal – Wallis test p= 0.088 at week 20, and p = 0.168 at week 45), and this increase was also observed for community size, which approaches that of the unwarmed control (Kruskal – Wallis test Control vs Disturbance + Immigration p=0.11, Control vs Disturbance p=0.0004, Disturbance vs Disturbance + Immigration p=0.013) (**Figure 3B**). This suggests that the dispersal treatment was effective in promoting the process of recovery in richness and community size. Importantly, Disturbance and Disturbance + Immigration mesocosms were not significantly different in either richness nor community size prior to the immigration event (Table S1 and S2) However, disturbed mesocosms did not completely recover richness to the level of the ambient Controls, even by week 45 (**Figure 2B**). Evenness followed the same overarching patterns as richness (**Figure 2CD**).

We compared community structure across treatments for the Total community dataset, rRNA gene; 14,159 OTUs) and the Active dataset (rRNA:rRNA gene > 1; 6,693 = OTUs). There were clear and consistent shifts in beta diversity in the disturbed mesocosms (n=9, inclusive of Disturbance and Disturbance + Immigration), as well as high reproducibility among replicates in community structure within treatments as shown by the overlap of symbols per treatment and timepoint in the ordination (**Figure 4**). As compared to the Controls, the disturbed mesocosms had increased betadispersion (variability in community structure) starting at week 6 onward, with the exception of week 10 (**Figure 5**). Over the experiment, disturbed mesocosms had distinct community structures compared to Control (disturbed v. Control PERMANOVA PsuedoF

= 63.87, Rsqr = 0.345, p=0.001 for Total communities, and PsuedoF=35.97, Rsqr=0.229, p=0.001 for Active communities, all timepoints). Control communities were relatively stable over the study, while disturbed communities changed directionally, and were significantly different from Control communities after a single week of warming (week 5 Control vs Disturbed PERMANOVA PsuedoF = 3.06, Rsqr= 0.218, p=0.001 for Total community and PsuedoF= 2.88, Rsqr=0.208, p=0.001 for Active community, Week 4 PERMANOVA p>0.05, Table S3). Disturbed communities continued to shift with temperature during the course of the experiment, and then shifted slightly back towards the Control after the stressor was released and Disturbance and Disturbance + Immigration communities had similar structures during the press (Table S4). Though no disturbed mesocosms fully recovered to overlap with the Control communities, the Disturbance + Immigration mesocosms were more similar to the Control than the Disturbance mesocosms without dispersal (Figures 2B, 3B, 4) . Across all treatments, Total communities and Active communities were synchronous in their temporal trajectories (Mantel R =0.943, p = 0.001 on 999 permutations; Protest Sum of Squares =0.238, R= 0.873, p=0.001), but there was higher betadispersion in the disturbed treatments for the Active communities (Comparing Total v. Active for disturbed mesocosms, Kruskal Wallis p=0.029). This suggests that there was Active community variability masked by the contributions of dead and dormant taxa to the Total community.

Replicate disturbed mesocosms (again, inclusive of Disturbance and Disturbance + Immigration) had highly reproducible responses during the press. They had high overlap in membership and overall synchronous trajectories (i.e. changes in community structure through

time), even after the immigration event at week 16 (33 of 36 PROTEST all R > 0.89 and false-discovery rate adjusted p-values < 0.05).

Resistance and resilience

For the Active community, we calculated resistance and resilience of the disturbed mesocosms relative to the Control using community divergence from the first sampling time (Week4, end of acclimatization period) as the reference (**Figure 6A**). Even in the Control communities, there was an initial drop in similarity between weeks 4 and 5, which we attribute to incomplete acclimatization and a bottle effect. However, after that, the Control communities remain relatively stable with no additional divergence, while the disturbed communities decrease to their maximum divergence at week 10 (60°C).

Disturbance + Immigration communities converge slightly after the dispersal event. Overall resistance was low (**Figure 6B**), and resilience reached its maximum, 0.41, in the immigration treatment between weeks 16 (the time point at which the thermal press was released) and the final week 45, but ranged from a minimum of 0.04 between week 16 and 20 in the Disturbance without immigration treatment (**Figure 6C-E**). Immigration enhanced resilience from week 16 to week 20 (Kruskal Wallis p value 0.034) and from week 16 to week 45 (Kruskal Wallis p value 0.083), but not from week 20 to 45, possibly because of insufficient power (Kruskal Wallis p value 0.180). Notably, there were only two Disturbance mesocosm replicates (out of five) that met the rarefaction threshold for week 45.

We wanted to assess the relative contributions of taxa that activate or inactivate after the disturbance subsides to the overall beta diversity (weeks 16-45). We also wanted to assess

391 the relative contributions of taxa that colonized after dispersal. We calculated the relative
392 contribution of activity dynamics by identifying taxa that switched between an active and
393 inactive state during secondary succession. We found that these dynamically active taxa
394 contributed 11.7% to 58.9% (median 28.6%) of the observed beta diversity, while immigrants
395 contributed 7.9% to 26.3% (median 14.7%) of the observed beta diversity during the same time
396 period**.**
397
398 *Activity dynamics of abundant taxa*
399 We investigated the activity dynamics of the top 50 most abundant taxa within the
400 Active communities, and distinguished taxa that became inactive (rRNA:rRNA gene < 1, white
401 cells in **Figure 7A**) from taxa that fell below detection (rRNA gene = 0, black cells in **Figure 7A**,
402 see Methods for details). Within this set of 50, we detected no purely resistant taxa that were
403 consistently active throughout the experiment. This finding agrees with the analyses showing
404 low resistance (**Figure 6B**) and substantial shifts in the disturbed communities (**Figure 5**). We
405 detected 17 taxa that were sensitive to the disturbance (**Figure 7B**). Sensitive taxa were active
406 prior to the warming but became inactive or dropped below detection during the warming, and
407 then did not reactivate. We also detected 19 transition taxa that were inactive prior to the
408 warming, active during the warming, and then became inactive after the stressor was released.
409 Because there was no external dispersal into the system, these thermotolerant taxa were likely
410 in the dormant pool of the soil. We could divide these responses generally into early and late
411 transition taxa. There were 6 early transition taxa that became active during week 5 or 6 of the

412 experiment, but then became inactive at weeks 10 and 14. There were also 13 late transition
413 taxa that remained inactive during weeks 5 and 6 but became active during weeks 10 and 14.
414 Among the top 50 Active taxa, we did not detect purely resilient taxa that were active
415 prior to the warming, became inactive during the warming, but then reactivated after the
416 return to ambient temperature. This suggests that dormancy strategies responsive to warming
417 were not a substantial contributor to member preservation, nor to eventual re-seeding.
418 Instead, opportunists and immigrants facilitated resilience in the mesocosms. The opportunists
419 were defined as inactive or below detection prior to and during the warming, but then
420 activated after the temperature returned, likely due to resuscitation, and there were five taxa
421 in this category. Eight immigrants were generally active prior to the warming, dropped to below
422 detection or became inactive during the warming, and then in the end, were active again only
423 in the Disturbance + Immigration treatment (and not in the Disturbance mesocosms without
424 immigration).
425
426
427 Discussion
428 Our results show that both dispersal and local dormancy dynamics, including activation
429 and inactivation, can contribute to overarching patterns of community resilience. The dispersal
430 event simulated in this experiment posed an optimistic scenario: well-mixed, control soils were
431 mixed into disturbed soils to maximize the volume of the disturbed soil that came into contact
432 with the inoculum. Regardless, by all metrics (beta diversity, alpha diversity, community size),
433 immigration was impactful. These data directly show that dispersal can augment resilience

434 towards recovery, supporting our hypothesis. Given that the influences of dispersal on
435 community assembly has been investigated previously (often indirectly for bacterial and
436 archaeal microbiomes, as inferred from the contributions of stochastic or neutral processes
437 e.g., [20,44–47]), this result is in agreement with the consensus of the literature that dispersal
438 and dispersal limitation can matter for assembly [48–50].
439 A new result is that local resuscitation also contributes to microbiome community
440 transitions during disturbance, and to resilience after the stress is released. Among the most
441 abundant taxa, there were near equal numbers of taxa that contributed to resilience via
442 resuscitation and to resilience via immigration. While, the influence of resuscitation on
443 resilience was not as impactful as that of dispersal (**Figure 6**), changes in activity dynamics
444 contributed 28.9% to the observed beta diversity during secondary succession. Therefore, both
445 mechanisms – local resuscitation and regional immigration – contribute to microbiome stability,
446 but potentially to different extents. The microbial dormant pool is important for maintaining
447 microbial diversity [51] and has evolutionary implications for traits that persist within inactive
448 populations [52]. To make more explicit the role of dormancy dynamics for community
449 disturbance responses (e.g., [53]), the phenomenon of the “storage effect” underpins modern
450 coexistence theory [54] and refers to the ability of competing species to coexist when their
451 growth and activities are separately partitioned over time, typically in dynamic environments
452 [55]. Given the severity of the thermal stressor in Centralia and in this experiment, our results
453 suggest that the soil microbial dormant pool is deep, in that it contains functionality for
454 distinctive conditions, like thermal stress, that are not within the expected range of

environmental variability. Our finding support other studies which have found thermophiles in unexpected environments such are arctic sediments and temperate soils [56–58].

Alternatively, it could be that, rather than local resuscitation, extremely rare but active taxa that were below the limits of detection grew rapidly and repopulated to become among the most active and abundant taxa. These data cannot rule out this possibility, and, if true, it would suggest an interesting role for release of rare taxa from competition (via death or inactivation of the competitors sensitive to the warming) in driving post-disturbance assembly. However, given that no resistant taxa were detected that could withstand the wide temperature range in the experiment, conditional rarity may be a less common scenario than opportunistic resuscitation.

Another goal of the experiment was to understand the reproducibility of member resuscitation given the press disturbance, and from the same soil. Because we observed high divergence in the hot soil communities in Centralia that was not attributable to any measured environmental variable, including temperature [20], we hypothesized that stochastic resuscitation could initiate priority effects (e.g., [10]), leading to divergent hot communities. However, we did not see the strongest differences in beta dispersion between Control and disturbed mesocosms until the press was subsiding (Weeks 15 and 16 in **Figure 5**). This, along with the overall strongly-correlated trajectories of disturbed community structures, suggest that the disturbance responses were consistent across disturbed mesocosms and do not support our hypothesis that priority effects (initiated by different resuscitating membership) determines community structure during the press. Therefore, we interpret that resuscitation in response to the thermal stress was largely deterministic, and that observed divergences among

hot soil communities in the field may be instead attributed to either differences local edaphic factors that were unmeasured, different structures of the underlying dormant pools, or stochasticity in regional dispersal during secondary succession.

Moving forward, there are several insights gleaned from this experiment. For soil, measuring dispersal in the field is difficult, given the various means by which microorganisms may arrive to a locality, including wind, ground water, and invertebrate vectors. Therefore, controlled experimentation is needed to quantify the contributions of dispersal to secondary succession. However, measuring activity dynamics and estimating the dormant pool of microbes in field samples, while imperfect, is possible [19,36,59,60]. Because our experiment suggests a role of resuscitation in determining the community that thrives during the disturbance, and also an influence of resuscitation for secondary succession towards recovery, we recommend to collect member activity data. More generally, routine characterization of the dormant pool of soil microbes, including its stability, diversity, and functions, can provide insights into the roles of these inactive taxa for disturbance responses.

Microbiome stability encompasses a progression along a trajectory, including a pre-disturbance community with a variance around a mean structure or a routine seasonal dynamic, a transition to an ephemeral community structure during the disturbance, and finally, after the disturbance is released, secondary succession towards either recovery or an alternative stable state. Longitudinal series of microbiome structure inclusive of all stages of this trajectory can be informative. Characterizing the full disturbance trajectory will allow for quantification of the different and potentially changing mechanisms that support stability (e.g., resuscitation, conditional rarity, immigration), and will facilitate prediction given new stressors.

In our experiment, one week of stress was sufficient to observe community sensitivity (by week 5, the control and the disturbance treatments were statistically different), but 29 weeks after the stress was released was not sufficient to observe complete recovery, though it seems that recovery is possible given the trajectory toward the controls. We expect that this time frame of response may be typical for many soils [61] and it can be used to inform future studies. Notably, while the objective of this study was to assess responses to elevated temperature, we expect that nutrient limitation was an outcome of the closed system experiment because we did not supplement it with resources. We expect microbial responses to nutrient limitation occurred in both control and disturbed mesocosms, and that nutrient limitation compounded with thermal stress in the disturbed mesocosms. Therefore, nutrient limitation may have contributed to incomplete recovery trajectory.

To conclude, this experiment shows both dispersal and dormancy dynamics can contribute to soil microbiome resilience in response to a press stress. Specifically, resuscitation of thermotolerant members contributed to microbiome transition during press, and then immigration provided a substantial boost to recovery beyond what was achieved with resuscitated opportunists. Because activity responses to the disturbance were consistent, these results suggest that predictive insights into microbiome resilience can be advanced more generally. We expect that accounting for mechanisms of local resuscitation and regional dispersal together will advance quantitative understanding of environmental microbiome stability.

521 Acknowledgements

522 This work was supported by the National Science Foundation under Grant No DEB#1749544.

523 This work was supported in part by Michigan State University through computational resources

524 provided by the Institute for Cyber-Enabled Research. We thank Johnathon Higgins for technical

525 assistance in the laboratory.

526

527 References

528 1. IPCC. 2014 *Climate Change 2014*. (doi:10.1017/CBO9781107415324)

529 2. Cavicchioli R *et al.* 2019 Scientists' warning to humanity: microorganisms and climate
530 change. *Nat. Rev. Microbiol.* (doi:10.1038/s41579-019-0222-5)

531 3. Singh BK, Bardgett RD, Smith P, Reay DS. 2010 Microorganisms and climate change:
532 Terrestrial feedbacks and mitigation options. *Nat. Rev. Microbiol.*
533 (doi:10.1038/nrmicro2439)

534 4. Pimm SL. 1984 The complexity and stability of ecosystems. *Nature* **307**, 321–326.

535 5. Allison SD, Martiny JBH. 2008 Resistance, resilience, and redundancy in microbial
536 communities. *Proc. Natl. Acad. Sci. U. S. A.* **105**, 11512–11519.

537 6. Shade A *et al.* 2012 Fundamentals of microbial community resistance and resilience.
538 *Front. Microbiol.* **3**, 417. (doi:10.3389/fmicb.2012.00417)

539 7. Kearns PJ, Shade A. 2018 Trait-based patterns of microbial dynamics in dormancy
540 potential and heterotrophic strategy: case studies of resource-based and post-press
541 succession. *ISME J.* (doi:10.1038/s41396-018-0194-x)

542 8. Orwin KH, Wardle DA. 2004 New indices for quantifying the resistance and resilience of
543 soil biota to exogenous disturbances. *Soil Biol. Biochem.* **36**, 1907–1912.
544 (doi:10.1016/j.soilbio.2004.04.036)

545 9. Leibold MA *et al.* 2004 The metacommunity concept: A framework for multi-scale
546 community ecology. *Ecol. Lett.* **7**, 601–613. (doi:10.1111/j.1461-0248.2004.00608.x)

547 10. Fukami T. 2015 Historical contingency in community assembly : integrating niches,
548 species pools, and priority effects. *Annu. Rev. Ecol. Evol. Syst.* **46**, 1–23.

(doi:10.1146/annurev-ecolsys-110411-160340)

11. Langenheder S, Berga M, Östman Ö, Székely AJ. 2012 Temporal variation of β-diversity and assembly mechanisms in a bacterial metacommunity. *ISME J.* **6**, 1107–1114. (doi:10.1038/ismej.2011.177)

12. Nemergut DR *et al.* 2013 Patterns and processes of microbial community assembly. *Microbiol. Mol. Biol. Rev.* **77**, 342–356. (doi:10.1128/MMBR.00051-12)

13. Lennon JT, Jones SE. 2011 Microbial seed banks: the ecological and evolutionary implications of dormancy. *Nat. Rev. Microbiol.* **9**, 119–130.

14. Hawkes C V., Keitt TH. 2015 Resilience vs. historical contingency in microbial responses to environmental change. *Ecol. Lett.* **18**, 612–625. (doi:10.1111/ele.12451)

15. Carini P, Marsden PJ, Leff JW, Morgan EE, Strickland MS, Fierer N. 2016 Relic DNA is abundant in soil and obscures estimates of soil microbial diversity. *Nat. Microbiol.* **2**, 16242. (doi:10.1101/043372)

16. Thompson LRLRLR *et al.* 2017 A communal catalogue reveals Earth's multiscale microbial diversity. *Nature* **551**. (doi:10.1038/nature24621)

17. Locey KJ, Lennon JT. 2016 Scaling laws predict global microbial diversity. *Proc. Natl. Acad. Sci. U. S. A.* **113**, 5970–5975. (doi:10.7287/peerj.preprints.1451v1)

18. Louca S, Mazel F, Doebeli M, Parfrey LW. 2019 A census-based estimate of earth's bacterial and archaeal diversity. *PLoS Biol.* (doi:10.1371/journal.pbio.3000106)

19. Blagodatskaya E, Kuzyakov Y. 2013 Active microorganisms in soil: Critical review of estimation criteria and approaches. *Soil Biol. Biochem.* **67**, 192–211. (doi:10.1016/j.soilbio.2013.08.024)

20. Lee S-H, Sorensen JW, Grady KL, Tobin TC, Shade A. 2017 Divergent extremes but convergent recovery of bacterial and archaeal soil communities to an ongoing subterranean coal mine fire. *ISME J.* **11**, 1447–1459. (doi:10.1038/ismej.2017.1)

21. Sorensen JW, Dunivin TK, Tobin TC, Shade A. 2018 Ecological selection for small microbial genomes along a temperate-to-thermal soil gradient. *Nat. Microbiol.*

22. Dunivin TK, Shade A. 2018 Community structure explains antibiotic resistance gene dynamics over a temperature gradient in soil. *FEMS Microbiol. Ecol.* **fiy016**. (doi:https://doi.org/10.1093/femsec/fiy016)

23. Kearns PJ, Shade A. 2017 Trait-based patterns of microbiome succession in dormancy and heterotrophic strategy. *PeerJ Prepr.* **5**.

24. Tobin-Janzen T *et al.* 2005 Nitrogen Changes and Domain Bacteria Ribotype Diversity in Soils Overlying the Centralia, Pennsylvania Underground Coal Mine Fire. *Soil Sci.* **170**, 191–201. (doi:10.1097/00010694-200503000-00005)

25. Nolter MA, Vice DH. 2004 Looking back at the Centralia coal fire: a synopsis of its present status. *Int. J. Coal Geol.* **59**, 99–106. (doi:10.1016/j.coal.2003.12.008)

26. Elick JM. 2011 Mapping the coal fire at Centralia, Pa using thermal infrared imagery. *Int. J. Coal Geol.* **87**, 197–203. (doi:10.1016/j.coal.2011.06.018)

27. Griffiths R, Whiteley A, O'Donnell A. 2000 Rapid method for coextraction of DNA and RNA from natural environments for analysis of Ribosomal DNA- and rRNA-Based Microbial Community Composition. *Appl. Environ. Microbiol.* **66**, 5488–5491. (doi:10.1021/ja00751a011)

28. Caporaso JG, Lauber CL, Walters WA, Berg-Lyons D, Lozupone CA, Turnbaugh PJ, Fierer N,

Knight R. 2011 Global patterns of 16S rRNA diversity at a depth of millions of sequences per sample. *Proc. Natl. Acad. Sci. U. S. A.* **108**, 4516.

29. Kozich JJ, Westcott SL, Baxter NT, Highlander SK, Schloss PD. 2013 Development of a dual-index sequencing strategy and curation pipeline for analyzing amplicon sequence data on the MiSeq Illumina sequencing platform. *Appl. Environ. Microbiol.* **79**, 5112–20. (doi:10.1128/AEM.01043-13)

30. Martin M. 2011 Cutadapt removes adapter sequences from high-throughput sequencing reads. *EMBnet.journal* **17**, 10-12. (doi:10.14806/ej.17.1.200)

31. Edgar RC. 2010 Search and clustering orders of magnitude faster than BLAST. *Bioinformatics* **26**, 2460–2461. (doi:10.1093/bioinformatics/btq461)

32. Edgar RC, Flyvbjerg H. 2014 Error filtering, pair assembly and error correction for next-generation sequencing reads. *Bioinformatics* **31**, 3476–3482. (doi:10.1093/bioinformatics/btv401)

33. Edgar RC. 2016 SINTAX: a simple non-Bayesian taxonomy classifier for 16S and ITS sequences. *bioRxiv* (doi:10.1101/074161)

34. Quast C, Pruesse E, Yilmaz P, Gerken J, Schweer T, Yarza P, Peplies J, Glöckner FO. 2013 The SILVA ribosomal RNA gene database project: Improved data processing and web-based tools. *Nucleic Acids Res.* **41**. (doi:10.1093/nar/gks1219)

35. Oksanen J, Kindt R, Legendre P, O'Hara B. 2006 The vegan Package for Community Ecology. , Ordination methods and other useful functions for.

36. Bowsher AW, Kearns PJ, Shade A. 2019 16S rRNA/rRNA Gene Ratios and Cell Activity Staining Reveal Consistent Patterns of Microbial Activity in Plant-Associated Soil.

mSystems **4**, e00003-19. (doi:10.1128/msystems.00003-19)

37. R Core Team. 2017 R: A Language and Environment for Statistical Computing.

38. Anderson MJ. 2001 A new method for non-parametric multivariate analysis of variance. *Austral Ecol.* **26**, 32–46.

39. Anderson MJ. 2005 Distance-Based Tests for Homogeneity of Multivariate Dispersions. *Biometrics* **62**, 245–253.

40. Wickham H. 2009 *ggplot2: Elegant graphics for data analysis*. New York: Springer-Verlag. See http://ggplot2.org.

41. Warnes GR *et al.* 2016 gplots: Various R Programming Tools for Plotting Data.

42. Shade A *et al.* 2014 Conditionally rare taxa disproportionately contribute to temporal changes in microbial diversity. *MBio* **5**, e01371-14. (doi:10.1128/mBio.01371-14)

43. Grady KL, Sorensen JW, Stopnisek N, Guittar J, Shade A. 2019 Assembly and seasonality of core phyllosphere microbiota on perennial biofuel crops. *Nat. Commun.* **19**. (doi:10.1038/s41467-019-11974-4)

44. Ferrenberg S *et al.* 2013 Changes in assembly processes in soil bacterial communities following a wildfire disturbance. *ISME J.* **7**, 1102–1111. (doi:Doi 10.1038/Ismej.2013.11)

45. Dini-Andreote F, Stegen JC, van Elsas JD, Salles JF. 2015 Disentangling mechanisms that mediate the balance between stochastic and deterministic processes in microbial succession. *Proc. Natl. Acad. Sci.* **112**, E1326–E1332. (doi:10.1073/pnas.1414261112)

46. Burns AR, Zac Stephens W, Stagaman K, Wong S, Rawls JF, Guillemin K, Bohannan BJ. 2016 Contribution of neutral processes to the assembly of gut microbial communities in the zebrafish over host development. *ISME J.* **10**, 655–664. (doi:10.1038/ismej.2015.142)

47. Zhou J *et al.* 2013 Stochastic assembly leads to alternative communities with distinct functions in a bioreactor microbial community. *MBio* (doi:10.1128/mBio.00584-12)

48. Evans S, Martiny JB, Allison SD. 2017 Effects of dispersal and selection on stochastic assembly in microbial communities. *ISME J.* **11**, 176–185. (doi:10.1038/ismej.2016.96)

49. Günther S, Faust K, Schumann J, Harms H, Raes J, Müller S. 2016 Species-sorting and mass-transfer paradigms control managed natural metacommunities. *Environ. Microbiol.* **18**, 4862–4877. (doi:10.1111/1462-2920.13402)

50. Nemergut DR *et al.* 2016 Decreases in average bacterial community rRNA operon copy number during succession. *ISME J.* **10**, 1147–1156. (doi:10.1038/ismej.2015.191)

51. Jones SE, Lennon JT. 2010 Dormancy contributes to the maintenance of microbial diversity. *Proc. Natl. Acad. Sci. U. S. A.* **107**, 5881–5886. (doi:10.1073/pnas.0912765107)

52. Shoemaker WR, Lennon JT. 2018 Evolution with a seed bank: The population genetic consequences of microbial dormancy. *Evol. Appl.* **11**, 60–75. (doi:10.1111/eva.12557)

53. Miller AD, Chesson P. 2009 Coexistence in disturbance-prone communities: how a resistance-resilience trade-off generates coexistence via the storage effect. *Am. Nat.* **173**, E30–E43. (doi:10.1086/597669)

54. Warner RR, Chesson PL. 1985 Coexistence mediated by recruitment fluctuations - a field guide to the storage effect. *Am. Nat.* **125**, 769–787.

55. Barabás G, D'Andrea R, Stump SM. 2018 Chesson's coexistence theory. *Ecol. Monogr.* (doi:10.1002/ecm.1302)

56. Hubert C *et al.* 2009 A constant flux of diverse thermophilic bacteria into the cold Arctic seabed. *Science (80-.).* **325**, 1541–1544. (doi:10.1126/science.1174012)

57. Portillo MC, Santana M, Gonzalez JM. 2012 Presence and potential role of thermophilic bacteria in temperate terrestrial environments. *Naturwissenschaften* **99**, 43–53. (doi:10.1007/s00114-011-0867-z)

58. Marchant R, Franzetti A, Pavlostathis SG, Tas DO, Erdbrugger I, Unyayar A, Mazmanci M a., Banat IM. 2008 Thermophilic bacteria in cool temperate soils: Are they metabolically active or continually added by global atmospheric transport? *Appl. Microbiol. Biotechnol.* **78**, 841–852. (doi:10.1007/s00253-008-1372-y)

59. Blazewicz SJ, Barnard RL, Daly R a, Firestone MK. 2013 Evaluating rRNA as an indicator of microbial activity in environmental communities: limitations and uses. *ISME J.* **7**, 2061–8. (doi:10.1038/ismej.2013.102)

60. Dlott G, Maul JE, Buyer J, Yarwood S. 2015 Microbial rRNA: RDNA gene ratios may be unexpectedly low due to extracellular DNA preservation in soils. *J. Microbiol. Methods* **115**, 112–120. (doi:10.1016/j.mimet.2015.05.027)

61. Shade A, Gregory Caporaso J, Handelsman J, Knight R, Fierer N. 2013 A meta-analysis of changes in bacterial and archaeal communities with time. *ISME J.* **7**, 1493–1506. (doi:10.1038/ismej.2013.54)

677 Figures

678 **Figure 1. Experimental design of the study.** At time 0 (indicated by the asterisk), reference
679 temperate soil (0-20 cm depth from surface) was homogenized and divided among fifteen 1 L
680 glass mesocosms that were maintained at ambient moisture through the experiment.
681 Nondestructive sampling of each mesocosm proceeded from week 4 onward as indicated by
682 the x-axis. Unwarmed Control mesocosms (solid gold line, n = 6) were maintained at 14°C,
683 which was ambient soil temperature at the time of collection. Disturbed mesocosms (dashed
684 blue line, n = 9, including Disturbance and Disturbance + Immigration groups) were acclimated
685 for four weeks at 14°C, increased to 60°C over two weeks, maintained at 60°C as a thermal
686 press disturbance for eight weeks, then decreased back to 14°C over two weeks, and finally
687 maintained for a total of 45 weeks. Four of the disturbance mesocosms received homogenized
688 soil slurry from Control mesocosms as a dispersal event at week 17, after the thermal press was
689 released (Disturbance + Immigration treatment; see methods). Note the break in the x-axis time
690 scale between weeks 20 and 45.
691
692 **Figure 2. Changes in alpha diversity over the disturbance experiment.** Alpha diversity was
693 assessed using operational taxonomic units clustered at 97% sequence identity, after 16S rRNA
694 gene sequencing and rarefaction to 50,000 sequences per sample. (A) Changes in the observed
695 no. OTUs (richness) in Control (gold, circles) and Disturbance (blue, squares and triangles)
696 mesocosms over the thermal press (weeks 4-16). (B) Changes in richness in Control (gold
697 circles), Disturbance (blue squares), and Disturbance + Immigration (pink triangles) mesocosms
698 over the recovery period, weeks 20-45. The Disturbance + Immigration mesocosms received a

699 dispersal event at week 17. (C) Changes in evenness over weeks 4-16. (D) Changes in evenness
700 over weeks 20-45. Asterisks indicate significant differences by a Kruskal Wallis test (n.s = not
701 significant; * p<0.1, ** p<0.01, *** p<0.001, with a Dunn correction for multiple comparisons in
702 B and D).
703
704 **Figure 3. Changes in community size over the disturbance experiment**. Community size was
705 estimated using qPCR of the 16S rRNA gene and standardized per gram of soil from which
706 nucleic acids were extracted. (A) Changes in the 16S rRNA gene copies in Control (gold, circles)
707 and disturbed (blue, squares and triangles) mesocosms over the thermal press (weeks 4-16). (B)
708 Changes in the 16S rRNA gene copies in Control, Disturbance (blue squares) and Disturbance +
709 Immigration (pink triangles) mesocosms over the recovery period, weeks 20-45. The
710 Disturbance + Immigration mesocosms received a dispersal event at week 17. Asterisks indicate
711 significant differences by a Kruskal Wallis test (n.s. = not significant, * p<0.1, ** p<0.01, ***
712 p<0.001, with a Dunn correction for multiple comparisons in B).
713
714 **Figure 4. Changes in beta diversity over the disturbance experiment.** Pairwise differences in
715 community structure was quantified using pairwise Bray-Curtis dissimilarity and then ordinated
716 using Principal Coordinates Analysis (PCoA). Time is shown by symbol size, and mesocosm
717 temperature is indicated by heat colors, with the brightest red indicating the warmest time
718 point. Control mesocosms are circles, Disturbance are squares, and Disturbance + Immigration
719 are triangles. (A) PCoA of the Total community, assessed using sequencing of the 16S rRNA
720 gene. (B) PCoA of the Active community, including only OTUs that had 16S rRNA:rRNA gene > 1.

721

722 **Figure 5. Changes in beta dispersion over the disturbance experiment.** Beta dispersion, an
723 indicator of variability in community structure, was quantified using the distance to the median
724 in ordination space (Figure 4), which was constructed based on Bray-Curtis dissimilarity. (A)
725 Changes in beta dispersion in Control (gold, circles) and Disturbance (blue, squares and
726 triangles) mesocosms over the thermal press (weeks 4-16). (B) Changes in beta dispersion in
727 Control, Disturbance (blue squares), and Disturbance + Immigration (pink triangles) mesocosms
728 over the recovery period, weeks 20-45. The Disturbance + Immigration mesocosms received a
729 dispersal event at week 17. Asterisks indicate significant differences with a Tukey's Honestly
730 Significant Difference post-hoc test (n.s. = not significant, * $p<0.1$, ** $p<0.01$, *** $p<0.001$).
731 Note differences in y-axis ranges between A and B.

732

733 **Figure 6. Resistance and resilience of soil mesocosm communities to a thermal press.** (A)
734 Temporal series of community divergence from pre-disturbance community (week 4) in Control
735 (gold solid line), Disturbance (blue short dashed line), and Disturbance + Immigration (pink long
736 dashed line) to calculate resistance and resilience. (B) Resistance of disturbed mesocosms at
737 week 10, the time point of maximum community change after the thermal press begins. (C-E)
738 Resilience of disturbed mesocosms without (-) and with (+) immigration, calculated after the
739 thermal press is released (week 16) for the (C) full recovery to week 45, (D) initial recovery to
740 week 20, and also for (E) long-term recovery from weeks 20 to 45. Asterisks indicate significant
741 differences by a Kruskal Wallis test (n.s. = not significant, * $p<0.1$).

742

Figure 7. The activity dynamics of the 50 most abundant taxa in response to the press disturbance. (A) Heatmap and dendrogram of abundant taxa reveal common patterns of detection and activity. Black cells are taxa that were undetected (coded as NA) in the 16S rRNA gene (DNA) community, and white cells are taxa that were detected in the DNA but had 16S rRNA:rRNA gene < 1 (inactive, coded as 0). The heat gradient indicates each taxon's abundance relative to its maximum observed in disturbance treated mesocosms during the experiment. Immigration is indicated for weeks 20 and 45 by minus (no) and plus (yes) signs. (B) Summary of activity response patterns to the disturbance of the top 50 taxa, including resistant, sensitive, early and late transition, resilient, opportunist, and immigrant taxa. Definitions of each of these categories of taxa are found in the main text.

Figure S1. Rarefaction curves for soil mesocosm microbial communities.

Figure S2. Taxon activity and abundance relationships. (A) Log10 relative abundance and log10 rRNA:rRNA gene ratio were inversely correlated. Each point is a different OTU detected in the dataset that had 16S rRNA:rRNA gene greater than or equal to 1. (B) Distribution of percent sample richness (No. OTUs detected, inclusive of DNA and RNA datasets) that were phantom taxa (16S rRNA detected but not 16S rRNA gene). (C) Distribution of percent RNA reads attributed to phantom taxa.

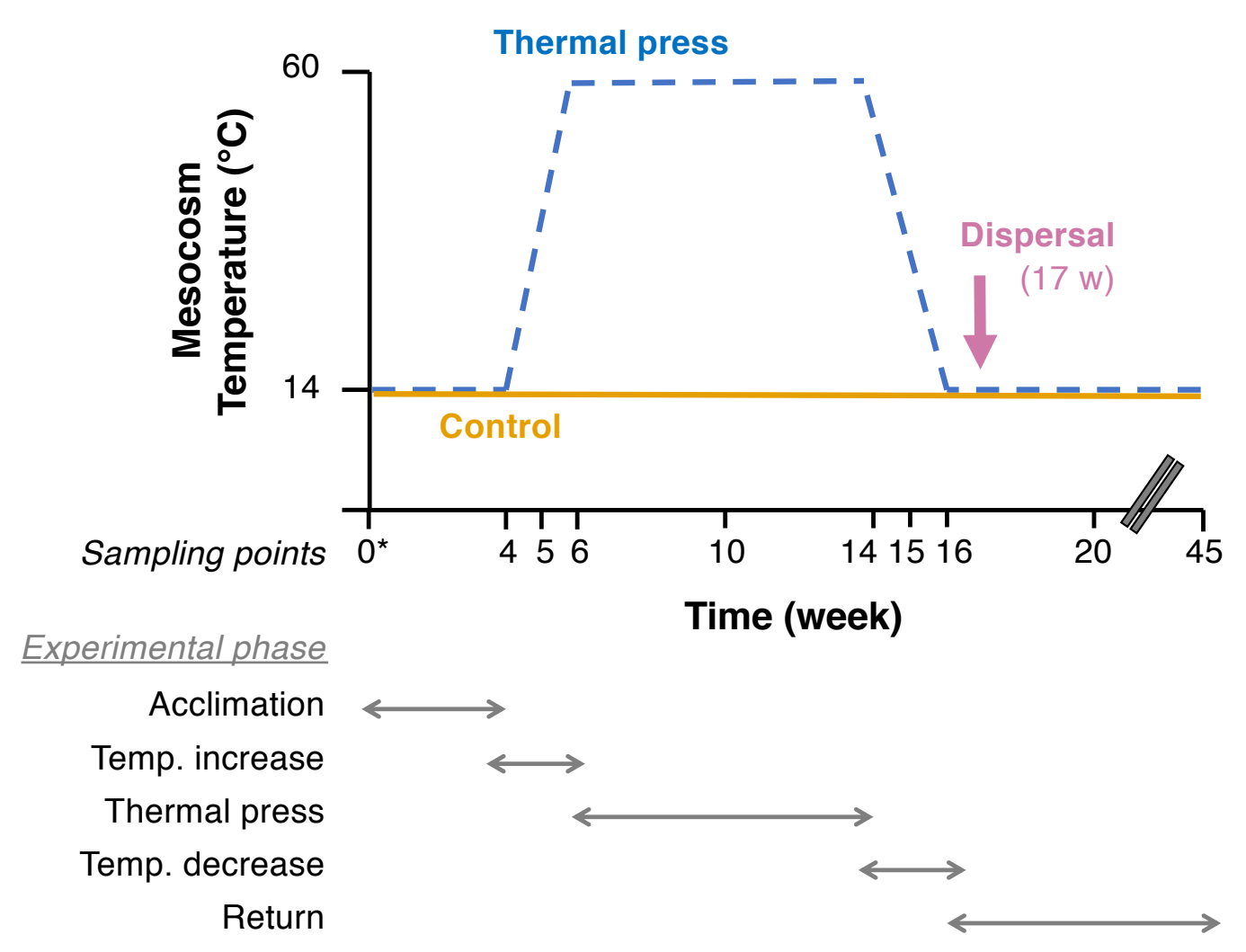
Thermal press
60
14
Mesocosm Temperature (°C)
Dispersal
(17 w)
Control
Sampling points
0*
4
5
6
10
14
15
16
20
45
Time (week)
Experimental phase
Acclimation
Temp. increase
Thermal press
Temp. decrease
Return

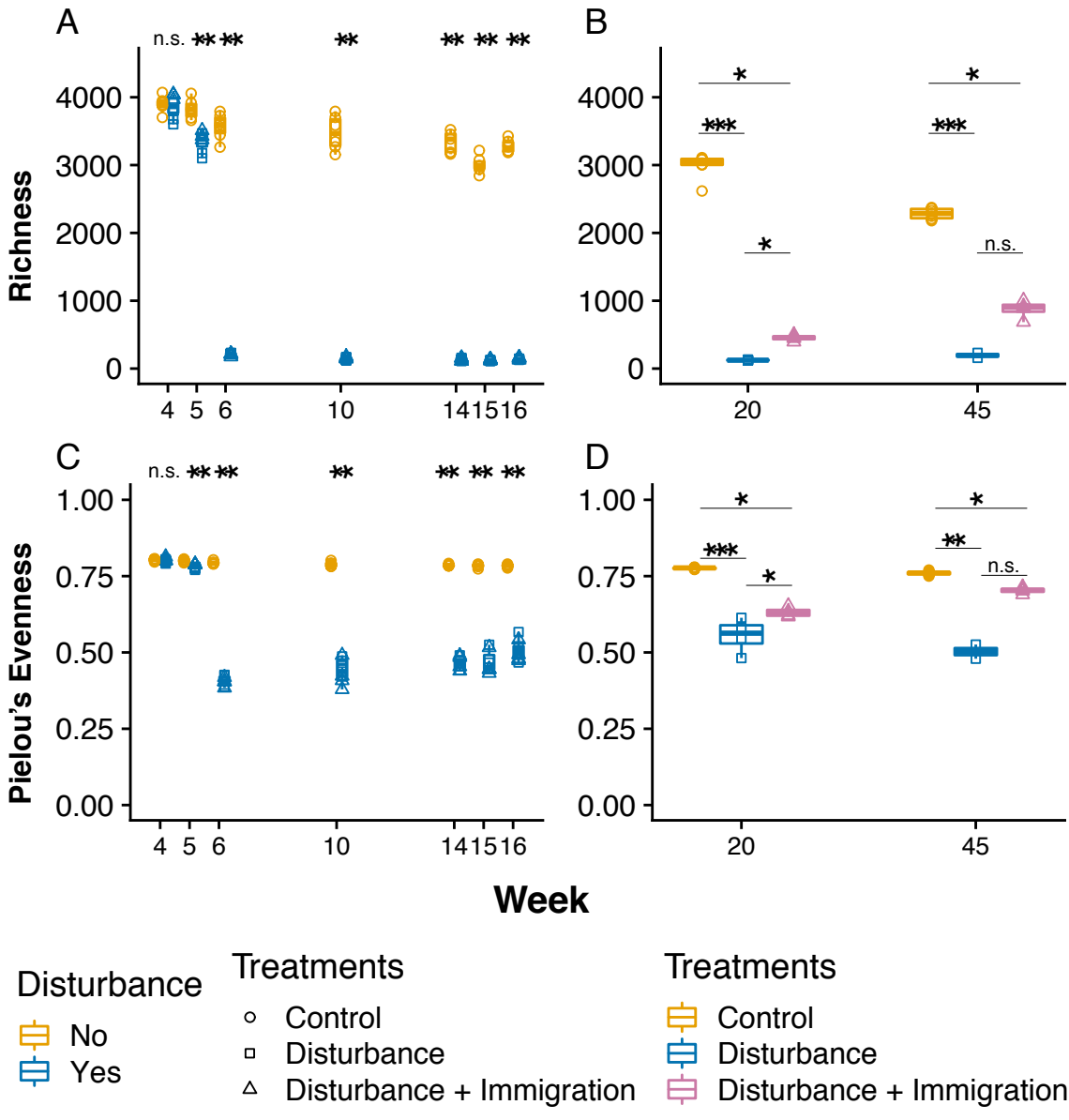
A
B
C
D
Richness
Pielou's Evenness
Week
n.s.
*
**
***
0
1000
2000
3000
4000
0.00
0.25
0.50
0.75
1.00
4
5
6
10
14
15
16
20
45
Disturbance
No
Yes
Treatments
Control
Disturbance
Disturbance + Immigration
Treatments
Control
Disturbance
Disturbance + Immigration

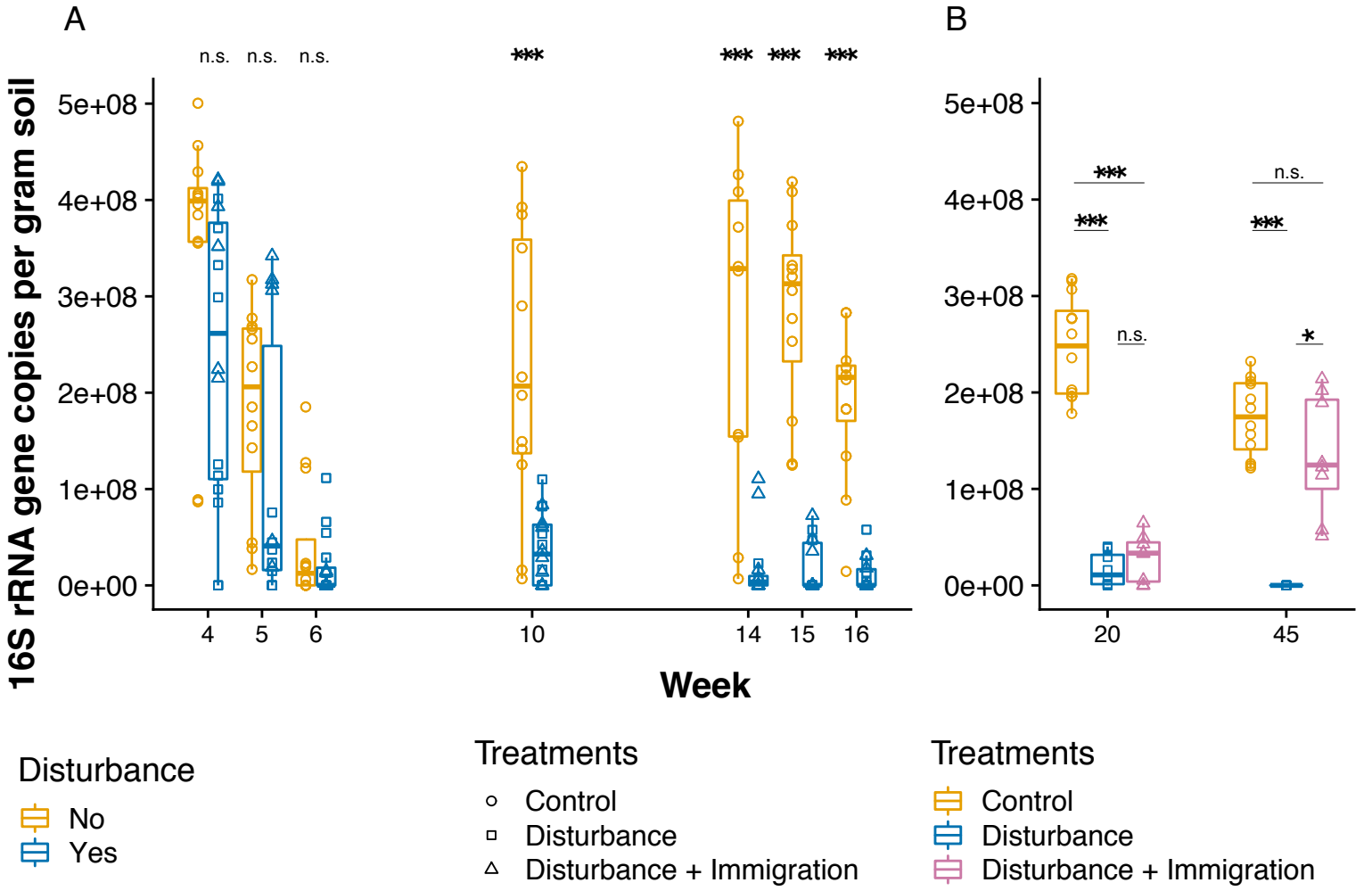
A
B
16S rRNA gene copies per gram soil
5e+08
4e+08
3e+08
2e+08
1e+08
0e+00
n.s.
n.s.
n.s.
***
***
***
***
4
5
6
10
14
15
16
Week
20
45
n.s.
*
Disturbance
No
Yes
Treatments
Control
Disturbance
Disturbance + Immigration
Treatments
Control
Disturbance
Disturbance + Immigration

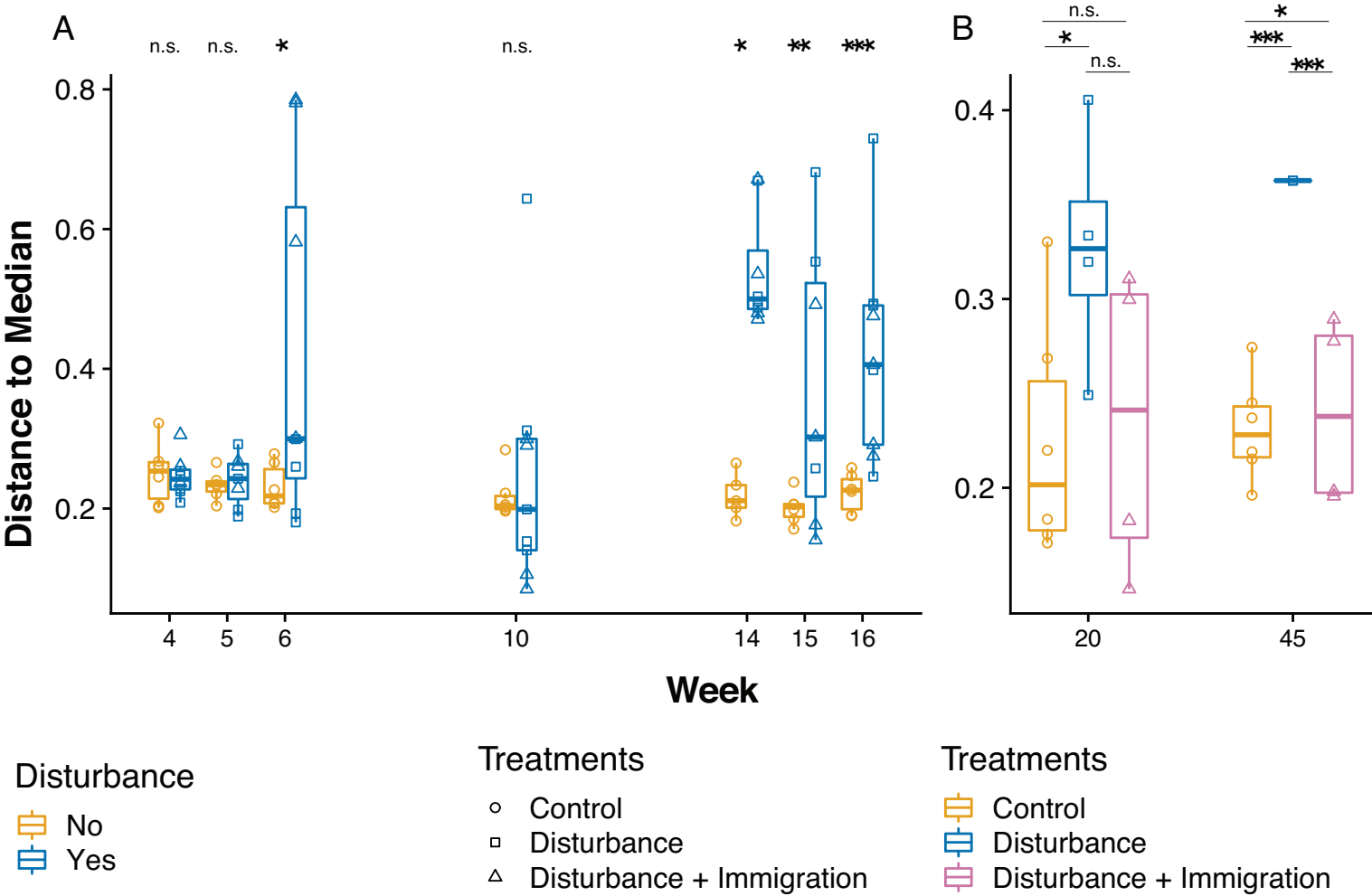
A
B
n.s.
n.s.
*
n.s.
*
**
***
n.s.
*
***
n.s.
***
Distance to Median
0.8
0.6
0.4
0.2
0.4
0.3
0.2
4
5
6
10
14
15
16
20
45
Week
Disturbance
No
Yes
Treatments
Control
Disturbance
Disturbance + Immigration
Treatments
Control
Disturbance
Disturbance + Immigration

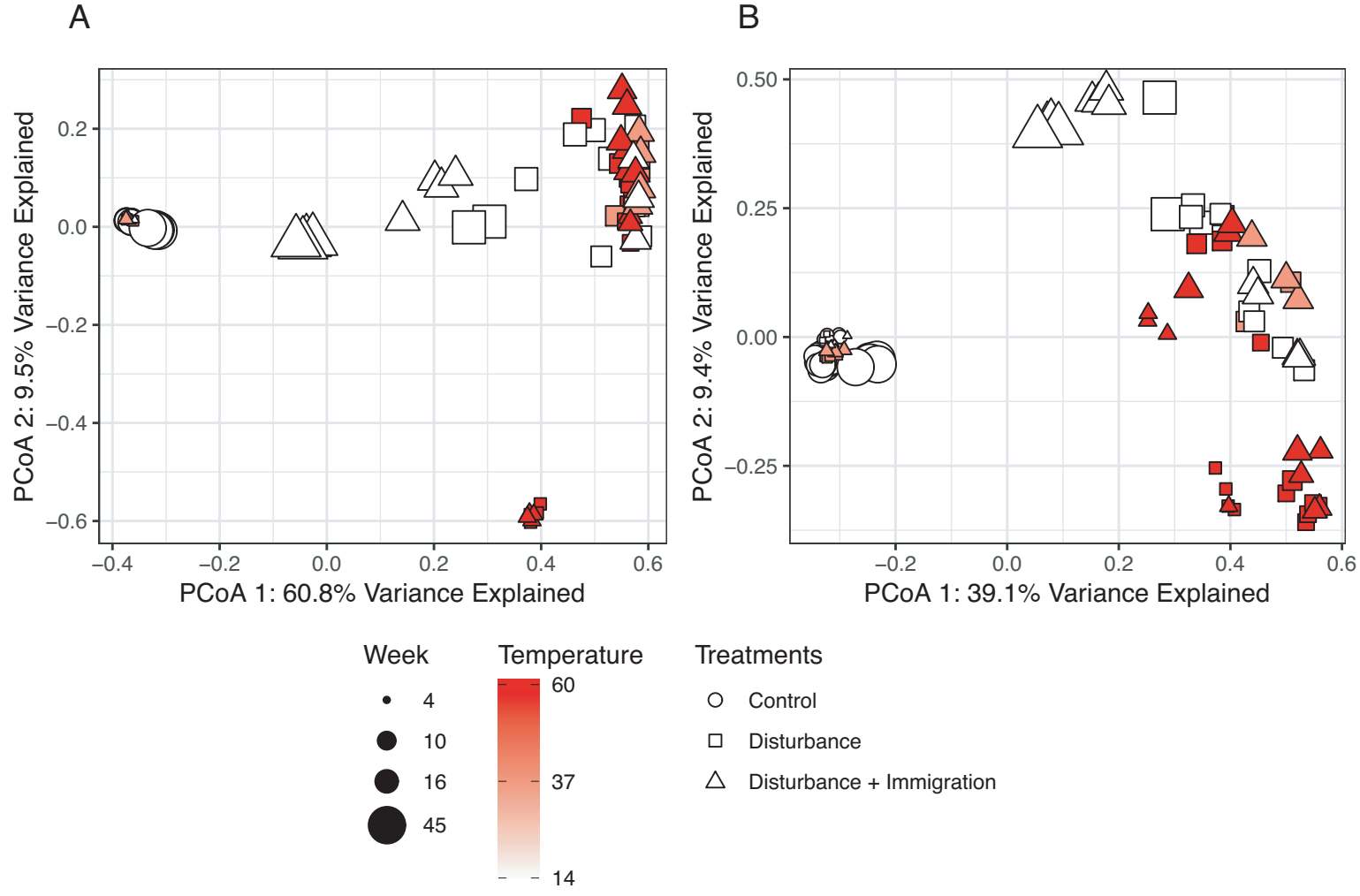
A
B
PCoA 2: 9.5% Variance Explained
PCoA 1: 60.8% Variance Explained
PCoA 2: 9.4% Variance Explained
PCoA 1: 39.1% Variance Explained
Week
4
10
16
45
Temperature
60
37
14
Treatments
Control
Disturbance
Disturbance + Immigration

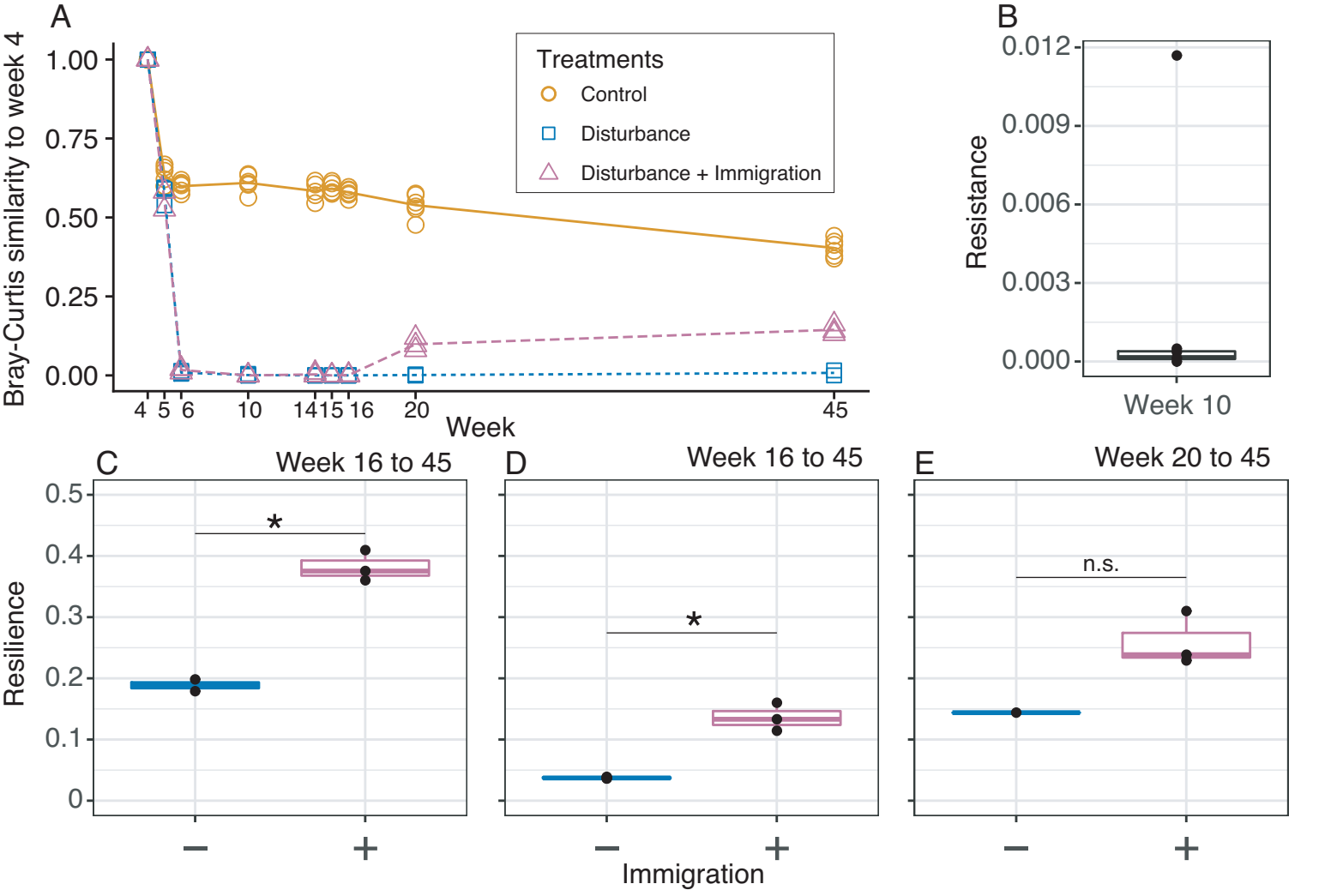
A
Bray-Curtis similarity to week 4
1.00
0.75
0.50
0.25
0.00
4 5 6 10 14 15 16 20 45
Week
Treatments
Control
Disturbance
Disturbance + Immigration
B
Resistance
0.012
0.009
0.006
0.003
0.000
Week 10
C
Week 16 to 45
Resilience
0.5
0.4
0.3
0.2
0.1
0
*
D
Week 16 to 45
*
E
Week 20 to 45
n.s.
−
+
Immigration

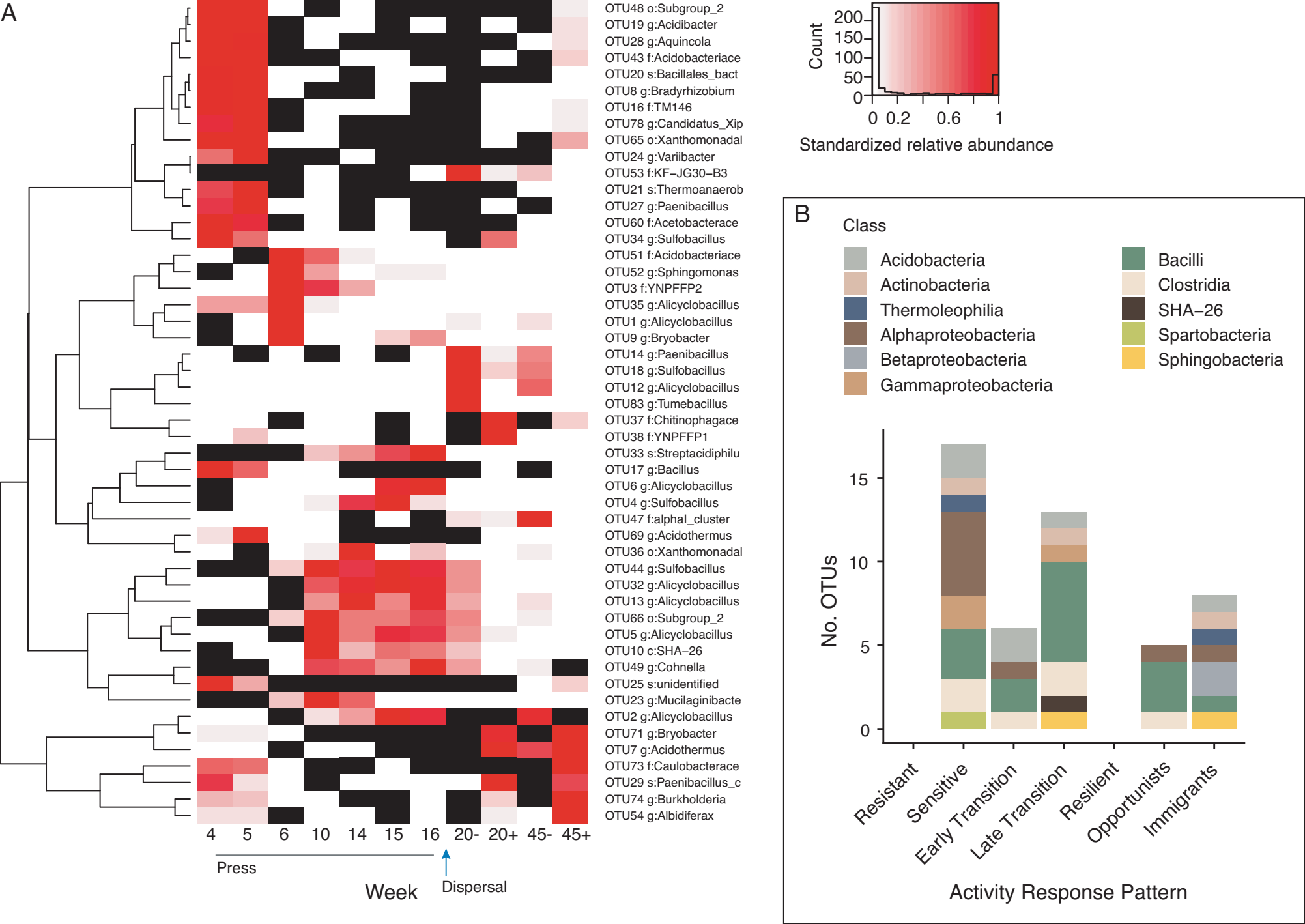
A
OTU48 o:Subgroup_2
OTU19 g:Acidibacter
OTU28 g:Aquincola
OTU43 f:Acidobacteriace
OTU20 s:Bacillales_bact
OTU8 g:Bradyrhizobium
OTU16 f:TM146
OTU78 g:Candidatus_Xip
OTU65 o:Xanthomonadal
OTU24 g:Variibacter
OTU53 f:KF−JG30−B3
OTU21 s:Thermoanaerob
OTU27 g:Paenibacillus
OTU60 f:Acetobacterace
OTU34 g:Sulfobacillus
OTU51 f:Acidobacteriace
OTU52 g:Sphingomonas
OTU3 f:YNPFFP2
OTU35 g:Alicyclobacillus
OTU1 g:Alicyclobacillus
OTU9 g:Bryobacter
OTU14 g:Paenibacillus
OTU18 g:Sulfobacillus
OTU12 g:Alicyclobacillus
OTU83 g:Tumebacillus
OTU37 f:Chitinophagace
OTU38 f:YNPFFP1
OTU33 s:Streptacidiphilu
OTU17 g:Bacillus
OTU6 g:Alicyclobacillus
OTU4 g:Sulfobacillus
OTU47 f:alphal_cluster
OTU69 g:Acidothermus
OTU36 o:Xanthomonadal
OTU44 g:Sulfobacillus
OTU32 g:Alicyclobacillus
OTU13 g:Alicyclobacillus
OTU66 o:Subgroup_2
OTU5 g:Alicyclobacillus
OTU10 c:SHA−26
OTU49 g:Cohnella
OTU25 s:unidentified
OTU23 g:Mucilaginibacte
OTU2 g:Alicyclobacillus
OTU71 g:Bryobacter
OTU7 g:Acidothermus
OTU73 f:Caulobacterace
OTU29 s:Paenibacillus_c
OTU74 g:Burkholderia
OTU54 g:Albidiferax
4 5 6 10 14 15 16 20- 20+ 45- 45+
Press
Week
Dispersal
Count
200
150
100
50
0
0 0.2 0.6 1
Standardized relative abundance
B
Class
Acidobacteria
Actinobacteria
Thermoleophilia
Alphaproteobacteria
Betaproteobacteria
Gammaproteobacteria
Bacilli
Clostridia
SHA−26
Spartobacteria
Sphingobacteria
No. OTUs
15
10
5
0
Resistant
Sensitive
Early Transition
Late Transition
Resilient
Opportunists
Immigrants
Activity Response Pattern

Supplementary Materials for "Dormancy dynamics and dispersal contribute to soil microbiome resilience" by JW Sorensen and A Shade

Supplementary Results

Relationships between taxon activity and abundance

The conventional thought is that relative abundance is the outcome of growth and therefore an indicator of fitness, and so high relative abundance is indicative of recent or current activity in the environment. However, we detected a weak, but statistically supported, inverse (log10) relationship between OTU 16S rRNA:rRNA gene ratio and relative abundance for those taxa with an rRNA:rRNA gene ratio >1 (**Figure S2A**, Pearson's R = -.14, $p < 0.0001$). This result is in agreement with other studies that have suggested that rare taxa may have high activity levels relative to their abundance in the community [42–46]. We present it here to be transparent that there are likely additional active but rare members that contribute to stability that have not been considered in our analyses.

The inverse relationship between activity and abundance could not include taxa that had RNA but no DNA detected (aka "phantom taxa", [44]) because they have an undefined 16S rRNA:rRNA gene ratio. We make clear that, to be conservative, phantom taxa (that have RNA but no DNA detected) were not included in the analyses, and that rare taxa that had high activity ratios were not included in the description of activity response patterns among the top 50 most abundant taxa. On balance, phantom taxa contributed proportionally few rRNA reads and few unique OTUs to the dataset (**Figure S2 B and C**). However, there were a few exceptions, including five samples that had >10% rRNA reads and > 50% of richness attributed

to phantom taxa. Four of these were from the Disturbance mesocosms at week 14 (peak-thermal press), and one sample was from week 16, at the end of the press. These samples also had relatively low richness and community size (**Figure 2** and **3**). We speculate that, by reducing community size and likely also total microbial biomass, the disturbance indirectly provoked relatively higher contributions by phantom taxa and conditionally rare taxa [47].

Supplementary Figures and Tables

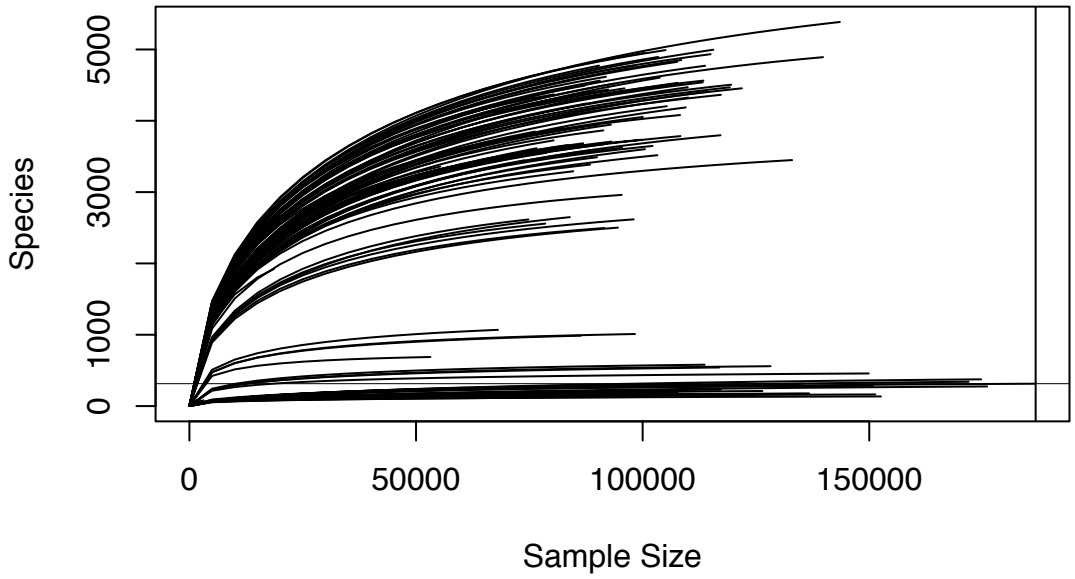

Figure S1: Rarefaction curves for soil mesocosm microbial communities.

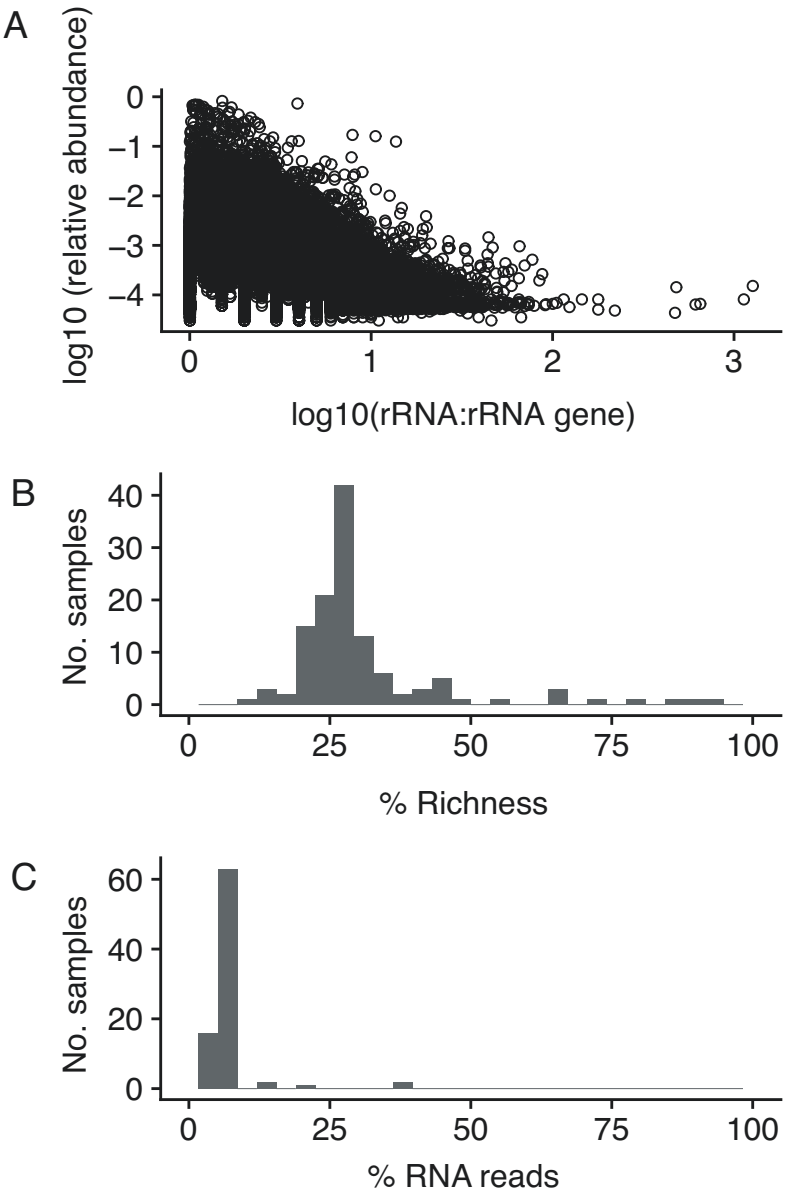

Figure S2. Taxon activity and abundance relationships. (A) Log10 relative abundance and log10 rRNA:rRNA gene ratio were inversely correlated. Each point is a different OTU detected in the dataset that had 16S rRNA:rRNA gene greater than or equal to 1. (B) Distribution of percent sample richness (No. OTUs detected, inclusive of DNA and RNA datasets) that were phantom taxa (16S rRNA detected but not 16S rRNA gene). (C) Distribution of percent RNA reads attributed to phantom taxa.

Table S1: Kruskal Wallis tests for Richness between Disturbance and Disturbance + Immigration mesocosms during the press

Week	KW rank sum statistic	p value
4	5.00	0.025
5	1.13	0.289
6	5.33	0.021
10	0.96	0.327
14	0.02	0.885
15	2.00	0.157
16	1.50	0.221

Table S2: Kruskal Wallis tests on community size between Disturbance and Disturbance + Immigration treatments during press

Week	KW rank sum statistic	p value
4	0.59	0.441
5	0.05	0.821
6	3.38	0.066
10	0.90	0.342
14	0.72	0.396
15	4.21	0.040
16	0.55	0.456

Table S3: ANOSIM tests on influence of disturbance on community structure

Week	ANOSIM R	P value
4	0.17	0.055
5	0.57	0.001
6	1.00	0.002
10	1.00	0.002
14	1.00	0.001
15	1.00	0.002
16	1.00	0.001
20	1.00	0.001
45	0.64	0.003

Table S4: ANOSIM results of community structure differences between Disturbance and Disturbance + Immigration mesocosms during the press.

Week	ANOSIM R	p value
4	0.54	0.038
5	0.15	0.222
6	-0.06	0.515
10	-0.05	0.63
14	0.07	0.449
15	0.20	0.196
16	0.04	0.359